



Published in final edited form as:

*Biosens Bioelectron.* 2009 July 15; 24(11): 3252–3257. doi:10.1016/j.bios.2009.04.010.

## Implantable Diagnostic Device for Cancer Monitoring

Karen D. Daniel<sup>a,j</sup>, Grace Y. Kim<sup>b,i,j</sup>, Christophoros C. Vassiliou<sup>c</sup>, Marilyn Galindo<sup>a</sup>, Alexander R. Guimaraes<sup>d,e</sup>, Ralph Weissleder<sup>d,e</sup>, Al Charest<sup>f</sup>, Robert Langer<sup>a,b,g,h</sup>, and Michael J. Cima<sup>h,i,\*</sup>

<sup>a</sup> Department of Chemical Engineering, Massachusetts Institute of Technology, Cambridge, MA

<sup>b</sup> Harvard-MIT Health Sciences & Technology, Cambridge, MA

<sup>c</sup> Department of Electrical Engineering & Computer Science, Massachusetts Institute of Technology, Cambridge, MA

<sup>d</sup> Center for Molecular Imaging Research, Massachusetts General Hospital, Boston, MA

<sup>e</sup> Center for Systems Biology, Massachusetts General Hospital, Boston, MA

<sup>f</sup> Department of Biology and Center for Cancer Research, Massachusetts Institute of Technology, Cambridge, MA and Department of Neurosurgery, Tufts Medical Center, Boston, MA

<sup>g</sup> Division of Biological Engineering, Massachusetts Institute of Technology, Cambridge, MA

<sup>h</sup> The David H. Koch Institute for Integrative Cancer Research, Massachusetts Institute of Technology, Cambridge, MA

<sup>i</sup> Department of Materials Science & Engineering, 77 Massachusetts Ave, Room 12-011, Cambridge, MA, 02139. Fax: 617-258-6936; Tel: 617-253-6877; E-mail: mjcima@mit.edu

### Abstract

Biopsies provide required information to diagnose cancer but, because of their invasiveness, they are difficult to use for managing cancer therapy. The ability to repeatedly sample the local environment for tumor biomarker, chemotherapeutic agent, and tumor metabolite concentrations could improve early detection of metastasis and personalized therapy. Here we describe an implantable diagnostic device that senses the local *in vivo* environment. This device, which could be left behind during biopsy, uses a semi-permeable membrane to contain nanoparticle magnetic relaxation switches. A cell line secreting a model cancer biomarker produced ectopic tumors in mice. The transverse relaxation time ( $T_2$ ) of devices in tumor-bearing mice was  $20 \pm 10\%$  lower than devices in control mice after one day by magnetic resonance imaging ( $p < 0.01$ ). Short term applications for this device are numerous, including verification of successful tumor resection. This may represent the first continuous monitoring device for soluble cancer biomarkers *in vivo*.

---

\* Correspondence should be addressed to M.J.C. (mjcima@mit.edu).

<sup>j</sup>These authors contributed equally to this work.

**Competing interests statement:** RL and MJC are directors at T<sub>2</sub> Biosystems, a company developing *in vitro* diagnostic assays.

**Publisher's Disclaimer:** This is a PDF file of an unedited manuscript that has been accepted for publication. As a service to our customers we are providing this early version of the manuscript. The manuscript will undergo copyediting, typesetting, and review of the resulting proof before it is published in its final citable form. Please note that during the production process errors may be discovered which could affect the content, and all legal disclaimers that apply to the journal pertain.

## 1. Introduction

Multiple clinical scenarios exist where short term sampling of the local tissue environment at the tumor site would be beneficial. A patient that has undergone tumor resection would benefit, for example, from sampling of fluids to confirm that all of the neoplastic tissue has been removed. Intraoperative parathyroid hormone (PTH) measurement is used in such a manner. Hyperparathyroidism, most often caused by parathyroid adenomas, can be surgically treated by removing the affected parathyroid glands. Serum PTH levels quickly decrease (within 5-10 minutes) once the hyper-secreting tissue has been removed and are, therefore, an indicator of whether additional removal of parathyroid tissue is needed (Sokoll et al., 2004, Lo et al., 2002). Serum biomarker concentrations may not be sensitive enough, however, to evaluate the successful removal of other types of tumors. Local biomarker concentrations are often a better indicator of the tumor environment (Baron et al., 2005, Sedlacek et al., 2002) and the device described here could be left behind during tumor resection to report on the local environment. Short term sensing of cancer biomarkers, several months after tumor resection, would be useful in detecting recurrence of fast growing brain gliomas. These new tumor growths are difficult to identify using standard imaging techniques, like MRI, because they are indistinguishable from benign lesions caused by chemoradiotherapy (Gomez-Rio et al., 2008, Gomez-Rio et al., 2004). Future research may yield devices that can be stable for extended periods of time *in vivo* which would be useful for development of new therapeutic agents and evaluation of targeted delivery modalities. They may also enable real-time personalized cancer treatment, featuring repeated tracking of treatment and monitoring of local reoccurrence with a single implant (Takeuchi et al., 2008, Chen, 2007, Agarwal et al., 2008, Carney, 2007).

One such device consists of nanoparticle magnetic relaxation switches (MRSw) which are contained within the diagnostic device by a semi-permeable membrane. Figure 1a is a photograph of a device used for *in vivo* sensing. The semi-permeable membrane that covers the reservoir allows cancer biomarkers or chemotherapeutic agents to diffuse into the device and interact with the MRSw but does not allow diffusion of the MRSw into the tissue environment. MRSw are magnetic nanoparticles with a superparamagnetic iron oxide core (about 4 nm in diameter) and a cross-linked dextran shell. Functional groups are used to covalently attach linking molecules, such as antibodies, to the MRSw surface. MRSw have been functionalized to detect a variety of molecules, such as peptides, oligonucleotides, nucleic acids, receptor ligands, proteins, small molecules and antibodies (Josephson et al., 1999, Josephson et al., 2001, Lewin et al., 2000, Perez et al., 2002, Sun et al., 2006). The MRSw aggregate in the presence of the analyte they were designed to detect and this aggregation causes a decrease in the transverse relaxation time ( $T_2$ ). MRI or nuclear magnetic resonance relaxometry can be used to quantify the  $T_2$  of the MRSw and determine if aggregation has occurred. These MRSw have been used extensively for *in vitro* agglutination assays where the MRSw and analyte solutions are mixed together. Continuous monitoring of glucose with MRSw contained within a dialysis membrane has also been demonstrated *in vitro* (Sun et al., 2006). Here we describe a device that will enable these MRSw to be used for *in vivo* sensing. Packaging the MRSw in our device addresses two key challenges related to using the MRSw *in vivo*: possible immune response to the protein modified nanoparticles, and  $T_2$  fluctuations due to changes in MRSw concentration. The semi-permeable membrane exposes the MRSw to analytes in the local environment but prevents the MRSw from invoking a possible immune response. The rigid device substrate provides a constant-volume reservoir so the concentration of MRSw remains constant. This allows any  $T_2$  changes to be attributed solely to aggregation of the nanoparticles.

We have demonstrated detection of a model cancer biomarker, the beta subunit of human chorionic gonadotrophin (hCG- $\beta$ ), in proof-of-principle *in vivo* sensing experiments. HCG- $\beta$  is a soluble biomarker that is elevated in testicular and ovarian cancer (Badgwell et al., 2007,

Duffy, 2001, Grossmann et al., 1995, Hoermann et al., 1992). Serum concentrations up to 16  $\mu\text{g/ml}$  were reported in one condition, persistent trophoblastic disease, whereas they are usually less than 0.005  $\mu\text{g/ml}$  in normal men and women (van Trommel et al., 2006). MRSw have been previously shown to detect 0.5 to 5  $\mu\text{g/mL}$  hCG- $\beta$  (Kim et al., 2007). Two populations of MRSw were prepared ( $C_{95}$  and  $C_{97}$ ), each conjugated with a different monoclonal antibody for hCG- $\beta$  (Fig. 1b). Aggregation occurs when both types of MRSw are present with either the hCG- $\beta$  subunit or the hCG dimer. *In vitro* device dose response and operation time were previously established (Supplemental Fig. 1). The high binding affinity of the antibodies favors irreversible MRSw. The signal measured is, thus, an integral of total exposure to the analyte over time and as such could be significantly more sensitive. The local concentration of hCG affects the rate of  $T_2$  change such that a low concentration of hCG is still expected to increase the measured signal, but at a slower rate than a higher concentration. *In vivo* performance was assessed using a commercially available human epithelial cell line (JEG-3) to produce ectopic tumors that secrete hCG in nude mice. Plasma hCG- $\beta$  concentrations were quantified with an enzyme-linked immunosorbent assay (ELISA). Implantation was performed when the plasma hCG- $\beta$  concentrations achieved the device detection limit of 0.5  $\mu\text{g/mL}$  (Daniel et al., 2007) at approximately two weeks (Fig. 2).

## 2. Materials and methods

### 2.1. Device fabrication

Cylinders of high density polyethylene (HDPE, 10 mm diameter) were cut from a 3 mm thick sheet to make the device substrate. The centers of the cylinders were drilled out to create a cup-shaped device with a reservoir that is 5 mm in diameter and 2.5 mm deep. A 1.5 mm hole was drilled through the bottom of the cup as a filling port. Double-sided pressure sensitive adhesive was used to attach the polycarbonate membrane (10 nm pores,  $6 \times 10^8$  pores/cm<sup>2</sup>, SPI Supplies) to the top of the device. Previous diffusion experiments showed that 10 nm pore membranes were able to restrict diffusion of the MRSw. The reservoir was filled with 50  $\mu\text{L}$  of a 1:1 mixture of CLIO-anti-hCG- $\beta_{95}$  and CLIO-anti-hCG- $\beta_{97}$  ( $C_{95}$  and  $C_{97}$  for short) nanoparticles (Kim et al., 2007) through the filling port, and it was then sealed with single-sided pressure sensitive adhesive. A photograph of an *in vivo* sensing device is shown in Fig. 1a. The devices were immediately placed in phosphate buffered saline (PBS) pH 7.4 with 0.1% bovine serum albumin (BSA) and 1% penicillin-streptomycin and kept at room temperature. Single-sided MR was used to quantify the  $T_{2,eff}$  of the MRSw in each device immediately after fabrication and again after 12 - 24 hours to confirm that the devices were not leaking (an increase in  $T_{2,eff}$  is correlated to a decrease in iron concentration).

### 2.2. Tumor induction

JEG-3 cells (ATCC) were propagated and subcultured according to the manufacturer's instructions until the time of tumor induction. The cells were then harvested and counted with a particle counter (Beckman Z1 Coulter Particle Counter) to determine the cell concentration. The cells were washed three times and re-suspended in sterile PBS to a concentration of  $10^7$  cells/mL. Equal volumes of cell solution and growth factor reduced Matrigel<sup>TM</sup> matrix (BD Biosciences) were mixed together. Mice were anesthetized with an intraperitoneal injection of ketamine (100 mg/kg) and xylazine (10 mg/kg). A 16 gauge needle was tunneled subcutaneously from the shoulder to the flank of the mouse, and 200  $\mu\text{L}$  of the cell mixture was slowly injected (total of  $10^6$  cells per mouse) in the flank of each female NCr nude mouse (Taconic) (n = 27). The skin around the needle tip was compressed and held while the needle was removed and for the next 30-45 s to allow the cell solution to solidify as a depot. Control mice (no tumors, n = 7) underwent the same subcutaneous injection procedure on both flanks, with a solution of equal volumes of sterile PBS and Matrigel<sup>TM</sup>. Retroorbital bleeding was performed periodically after tumor induction. Mice were anesthetized with continuous 1-4%

isoflurane/oxygen inhalation, and the blood was collected in serum gel tubes (Sarstedt). The samples were centrifuged at 13,000 rpm for 5 minutes and then frozen for later analysis. Plasma hCG concentrations were determined using an ELISA kit (United Biotech Inc). The assay was performed according to the manufacturer's instructions using dilutions as necessary in the provided assay buffer. Device implantation was performed when a sharp increase in either tumor size or plasma hCG concentration was observed, between 13 to 19 days after tumor cell injection. All work involving mice was performed according to the policies of the Massachusetts Institute of Technology Committee on Animal Care. Mice were housed in autoclaved cages and had access to autoclaved food and water *ad libitum*.

### 2.3. Device implantation

Mice were anesthetized with an intraperitoneal injection of ketamine (100 mg/kg) and xylazine (10 mg/kg). Preemptive analgesics (buprenorphine, 0.1 mg/kg) were administered subcutaneously before the first incision. Mice with tumors (n = 27) received a dorsal midline incision, and blunt dissection was used to tunnel subcutaneously to the tumor site and create a pocket for the device. Mice without tumors (n = 7) also received a dorsal midline incision and blunt dissection was used to create a pocket on each flank (two devices per mouse). All devices were placed in the pocket with the membrane facing the muscular layer and the incision was closed with silk sutures. Mice were monitored daily for signs of distress, infection, or excessive tumor burden.

### 2.4. *Ex vivo* transport studies

Devices for *ex vivo* diffusion studies were similar to those described above but had a ring-shaped polyethylene substrate (10 mm inner diameter). The devices were filled with a PBS, 0.1% BSA, 1% penicillin-streptomycin solution and implanted subcutaneously in the flank of a female NCR nude mouse (Taconic) for one week (n = 3) or one month (n = 6). The device implantation procedure was the same as described above. The pressure sensitive adhesive was removed after explantation and the device was placed in a side-by-side diffusion cell (PermeGear) to quantify diffusion of <sup>14</sup>C-dextran (40 kDa, Sigma-Aldrich) through the membrane. Methods for diffusion experiments using side-by-side diffusion cells were previously described (Daniel et al., 2007). Three of the one month devices showed a dramatic increase in the analyte diffusion rate, indicating the presence of a defect in the membrane. These devices were excluded from the apparent permeability ( $P_{app}$ ) analysis, resulting in n = 3 for the  $P_{app}$  calculations.

### 2.5. MR imaging

Mice scheduled for MR imaging were transported to the Center for Molecular Imaging Research (CMIR) at Massachusetts General Hospital (MGH) after they awoke from anesthesia from the device implantation surgery (n = 6). They were imaged on day one and day four post device implantation, and subsequently transported to MIT so the devices could be explanted and measured on the single-sided MR. MRI was performed at 7 T on a Bruker imaging system (Pharmascan). Animals were anesthetized during imaging with 1-1.5% inhaled isoflurane, and monitored during imaging with respiratory monitoring. Imaging protocols included a Tri-plane and axial RARE localizer. Multi-slice multiecho (MSME)  $T_2$ -weighted imaging was performed utilizing the following parameters: Flip angle = 90°; Matrix size (128 × 184); TR = 2330 ms.; TE = 16 equally spaced echoes at 8.8 ms intervals ranging from 8.8 ms to 141 ms; field of view (FOV) = 4 × 4 cm, slice thickness = 1mm.  $T_1$ -weighted imaging was performed utilizing the following parameters: Flip angle = 90°; Matrix size (192 × 256); TR = 700 ms; TE = 14 ms; field of view (FOV) = 4 × 4 cm, slice thickness = 1mm. Region of interest analysis was performed and  $T_2$  fit by using a mono-exponential fitting algorithm for the multi-TE data (Osirix). ROI incorporating the center 2-3 slices of the device were analyzed. The fitting of

the  $T_2$  was modified by subtracting the mean background noise, and only points above this mean baseline threshold were used for the fit.

## 2.6. Single-sided MR

All devices were explanted two to four days post implantation and a  $T_{2,eff}$  measurement was immediately made using a single-sided NMR probe (Profile NMR MOUSE, ACT Center for Technology, Aachen, Germany). The explanted devices were individually positioned over the sensitive volume. The sensitive volume of the probe was located 2 mm above the center of the probe surface. The probe has a field strength of 0.43 T and a static field gradient of 15 mT/mm. It was maintained at 25°C using a circulating water bath. The similarity in magnitude between  $T_2$  measured by MRI and  $T_{2,eff}$  measured by single-sided MR is coincidental. A Minispec spectrometer (Bruker Optics) was used for pulse sequence generation and data acquisition.  $T_{2,eff}$  was measured using a 2000-echo CPMG pulse sequence with TE = 0.035 ms and TR = 1 s. The data were averaged over 48 scans. The measurements took approximately one minute per sample. The echo peak intensities were fit to the equation  $I = I_0 e^{-t/T_2}$  using a custom script running on MATLAB (The Mathworks).

## 2.7. Statistical analysis

F-tests were performed to compare variances of the control and tumor mice. Student's t-tests (one tail, equal or unequal variances depending on F-test values) were used to determine statistical significance. All values reported are mean +/- s.d. Error bars represent s.d. unless otherwise noted.

## 3. Results and discussion

### 3.1. *Ex vivo* transport

*Ex vivo* transport studies were performed to determine if adsorption of biomolecules would significantly affect analyte diffusion into the device. Diffusion of several model analytes, including hCG- $\beta$ , through polycarbonate membranes (10 nm pores) in phosphate buffered saline (PBS) with 0.1% bovine serum albumin (BSA) has been quantified previously (Daniel et al., 2007). Polycarbonate is a common material in medical devices and is considered biocompatible (Kessler et al., 2003, Viville et al., 1996) but adsorption of biomolecules to the nanoporous membranes due to implantation or incubation in serum containing media could reduce the pore size and hinder or completely prevent analyte diffusion through the membrane over time (Wisniewski et al., 2000). *Ex vivo* diffusion studies have shown that there is no noticeable decrease in analyte transport after the membranes have been implanted for up to one month. PBS-filled devices were implanted subcutaneously in mice for conditioning, then explanted and placed in a side-by-side diffusion chamber. The apparent permeability ( $P_{app}$ ) for the analyte (dextran, 40 kDa) through the conditioned membranes (one week: 3.0 +/- 0.5  $\mu\text{m}/\text{min}$ , n=3, one month: 2.9 +/- 0.2  $\mu\text{m}/\text{min}$ , n = 3) was approximately the same as the  $P_{app}$  for fresh membranes (2.81 +/- 0.07  $\mu\text{m}/\text{min}$ , n = 3) (Daniel et al., 2007) (p = 0.7 for one week, p = 0.4 for one month). These results indicate that while there may be some adsorption of biomolecules to the pore walls, the pores are not occluded and the diffusion of small molecules through the pores is not hindered. There is no significant effect on analyte transport into the device for the implantation duration reported here. The higher variability in the  $P_{app}$  of the conditioned membranes may be caused by manipulation of the membranes during the device fabrication and implantation process (Supplemental Fig. 2). Future studies will examine the effects of longer implantation times and fibrous capsule formation on membrane performance. Recent work with a silicon device gives promising evidence that a fibrous capsule may not significantly hinder protein transport up to 6 months in beagle dogs (Prescott et al., 2006).

### 3.2. *In vivo* sensing

Proof-of-principle *in vivo* sensing experiments were performed in a mouse model. High density polyethylene (HDPE) devices were made with a 5 mm inner diameter and 2.5 mm deep reservoir covered with a polycarbonate membrane (Fig 1a). The reservoir was filled with a MRSw solution. Mice were divided into two main groups: with a tumor (n = 27) and without a tumor (n = 7). Mice with tumors received one device, implanted subcutaneously near the tumor site once the plasma hCG concentrations began increasing. Mice without tumors received two devices, one on each flank. All the devices were filled with the same concentration of non-functionalized MRSw or MRSw functionalized to detect hCG.

Two techniques were used to quantify the transverse relaxation time of the MRSw in the device: MRI (reported as  $T_2$ ) and single-sided magnetic relaxometry (MR) (reported as  $T_{2,eff}$ ). A benefit of MRI is that it allows for live animal imaging, so the same device can be imaged multiple times. Single-sided MR requires the device to be explanted, so the  $T_{2,eff}$  can only be quantified at one time point using this technology. MRI is more time and cost-intensive than single-sided MR, however, so a subset of animals were chosen for MR imaging one day and four days after implantation, while all devices were analyzed with single-sided MR at explant. Four mice with tumors and two without tumors underwent MRI. Mice without tumors received a device on each flank, so there were four devices in each group. The imaging time points were chosen based upon the measured  $P_{app}$  of hCG through the polycarbonate membrane and the kinetics of aggregation for the MRSw. The analyte concentration in the reservoir was calculated to be more than 95% of the equilibrium concentration at one day (Daniel et al., 2007). This calculation assumes an infinite source of hCG, meaning that the concentration of hCG outside the reservoir remains constant. The infinite source assumption may not be valid *in vivo* and the time required to reach an equilibrium concentration may increase. The kinetic behavior of MRSw aggregation is another factor that could increase the time needed to see a decrease in  $T_2$ , as it continues to decrease for approximately 24 hours after mixing the analyte and MRSw solutions (Supplemental Fig. 3). The imaging session on day four was selected to allow for longer diffusion and aggregation times.

### 3.3. MRI detection

Figs. 3a-d shows examples of the type of MRI images obtained. Superimposed over each device is a pseudo-colored map that represents the  $T_2$  within the device. The  $T_2$  of the control device did not change from day one (Fig. 3a) to day four (Fig. 3b). The  $T_2$  of the device implanted near a tumor decreased from day one (Fig. 3c) to day four (Fig. 3d) and was lower than the control device on both days, indicating the presence of hCG at the tumor site. Fig. 3e shows that  $T_2$  of the control devices (no tumor present) were approximately constant over the two imaging time points.  $T_2$  of the sample devices were all lower than the control devices on day one and an even larger decrease in  $T_2$  was observed on day four. The mean  $T_2$  of the control devices (n = 4) was 34 +/- 2 ms on day one and 36 +/- 2 ms on day four. The mean  $T_2$  of the sample devices (n = 4) was 26 +/- 4 ms on day one and 19 +/- 3 ms on day four. The decrease in  $T_2$  of the sample devices compared to the control devices is statistically significant (Student's t-test, one tail, unequal variances) for both time points (p = 0.009 day one, p =  $4 \times 10^{-5}$  day four), suggesting that sufficient hCG had diffused into the reservoirs after one day to cause MRSw aggregation.

### 3.4. Single-sided MR detection

Single-sided MR was used to measure the  $T_{2,eff}$  of all devices at explant. Furthermore, devices filled with un-functionalized MRSw were implanted in mice with and without tumors as an additional control to test that the decrease in  $T_{2,eff}$  seen in devices filled with functionalized MRSw and implanted near a tumor site was indeed due to the presence of hCG, not some other effect of implantation near the tumor. Fig. 4 shows the mean  $T_{2,eff}$  of each group as quantified

by single-sided MR. Only mice with tumors and devices filled with MRSw functionalized to detect hCG showed a statistically significant ( $p = 3 \times 10^{-10}$ ) decrease in  $T_{2,eff}$  ( $33 \pm 2$  ms,  $n = 19$ ) compared to the same MRSw in devices implanted in mice without tumors ( $T_{2,eff} = 37.6 \pm 0.3$  ms,  $n = 8$ ). There was no statistically significant difference ( $p = 0.3$ ) in  $T_{2,eff}$  between the control mice ( $T_{2,eff} = 39.0 \pm 0.6$  ms,  $n = 6$ ) and sample mice ( $T_{2,eff} = 38.9 \pm 0.5$  ms,  $n = 8$ ) when the devices were filled with un-functionalized MRSw. Thus, the decrease in  $T_{2,eff}$  is caused by hCG induced aggregation of the nanoparticles functionalized to detect hCG.  $T_{2,eff}$  of individual devices is shown in Supplemental Figs. 4 and 5. Estimated area under the curve (AUC) of hCG did not correlate with the measured  $T_{2,eff}$ , but this is not surprising as systemic concentrations are not expected to accurately reflect the local concentration experienced by the device (Supplemental Fig. 6). The size of the mouse model was prohibitive for obtaining the local hCG concentration in the extracellular space. Future studies in a larger animal model will test the correlation between local hCG concentrations from repeated needle biopsy with each MRI measurement.

## 4. Conclusions

This work demonstrates the feasibility of MRSw-based devices for short term applications, such as verification of successful tumor resection, and represents the first continuous monitoring device of soluble cancer biomarkers *in vivo*. The device described here could also be used for *in vivo* sensing of chemotherapeutic agents or metabolites simply by changing the MRSw contained within the device. Long term use of such implanted sensors will require demonstration of *in vivo* stability for periods exceeding one month. If necessary, long term stability of the MRSw at 37°C may be improved by adding PEG as a linker when attaching the antibodies to the surface of the MRSw (Yuan et al., 2008) or by adding hydrophobic mutations or disulfide bonds to the antibody (Frokjaer and Otzen, 2005).

## Supplementary Material

Refer to Web version on PubMed Central for supplementary material.

## Acknowledgments

This work was supported by NCI Centers of Cancer Nanotechnology Excellence No. 5 U54 CA119349-12 grant and NSF Division of Materials Research Award No. 0746264. We would like to acknowledge Stephen Woolfenden for assistance with *in vivo* studies and Lee Josephson at CMIR for assistance with MRSw.

## References

- Agarwal PK, Black PC, Kamat AM. World Journal of Urology 2008;26:39–44. [PubMed: 18092171]
- Badgwell D, Lu Z, Cole L, Fritsche H, Atkinson EN, Somers E, Allard J, Moore RG, Lu KH, Bast RC. Gynecologic Oncology 2007;106:490–497. [PubMed: 17532030]
- Baron AT, Boardman CH, Lafky JM, Rademaker A, Liu DC, Fishman DA, Podratz KC, Mailhe NJ. Cancer Epidemiology Biomarkers & Prevention 2005;14:1583–1583.
- Carney WP. Expert Review of Molecular Diagnostics 2007;7:309–319. [PubMed: 17489737]
- Chen ZG. Current Cancer Drug Targets 2007;7:613–622. [PubMed: 18045066]
- Daniel KD, Kim GY, Vassiliou CC, Jalali-Yazdi F, Langer R, Cima MJ. Lab on a Chip 2007;7:1288–1293. [PubMed: 17896012]
- Duffy MJ. Critical Reviews in Clinical Laboratory Sciences 2001;38:225–262. [PubMed: 11451209]
- Frokjaer S, Otzen DE. Nature Reviews Drug Discovery 2005;4:298–306.
- Gomez-Rio M, Rodriguez-Fernandez A, Ramos-Font C, Lopez-Ramirez E, Llamas-Elvira JM. European Journal of Nuclear Medicine and Molecular Imaging 2008;35:966–975. [PubMed: 18172642]

- Gomez-Rio M, Torres DMD, Rodriguez-Fernandez A, Llamas-Elvira JM, Lozano SO, Font CR, Ramirez EL, Katati M. *European Journal of Nuclear Medicine and Molecular Imaging* 2004;31:1237–1243. [PubMed: 15133633]
- Grossmann M, Hoermann R, Gocze PM, Ott M, Berger P, Mann K. *European Journal of Clinical Investigation* 1995;25:867–873. [PubMed: 8582453]
- Hoermann R, Gerbes AL, Spoettl G, Jungst D, Mann K. *Cancer Research* 1992;52:1520–1524. [PubMed: 1540961]
- Josephson L, Perez JM, Weissleder R. *Angewandte Chemie-International Edition* 2001;40:3204–+.
- Josephson L, Tung CH, Moore A, Weissleder R. *Bioconjugate Chemistry* 1999;10:186–191. [PubMed: 10077466]
- Kessler L, Legeay G, Coudreuse A, Bertrand P, Poleunus C, Eynde XV, Mandes K, Marchetti P, Pinget M, Belcourt A. *Journal of Biomaterials Science-Polymer Edition* 2003;14:1135–1153. [PubMed: 14661884]
- Kim GY, Josephson L, Langer R, Cima MJ. *Bioconjugate Chemistry* 2007;18:2024–2028. [PubMed: 17892270]
- Lewin M, Carlesso N, Tung CH, Tang XW, Cory D, Scadden DT, Weissleder R. *Nature Biotechnology* 2000;18:410–414.
- Lo CY, Luk JM, Tam SC. *Annals of Surgery* 2002;236:564–569. [PubMed: 12409661]
- Perez JM, Josephson L, O'Loughlin T, Hogemann D, Weissleder R. *Nature Biotechnology* 2002;20:816–820.
- Prescott JH, Lipka S, Baldwin S, Sheppard NF, Maloney JM, Coppeta J, Yomtov B, Staples MA, Santini JT. *Nature Biotechnology* 2006;24:437–438.
- Sedlaczek P, Frydecka I, Gabrys M, van Dalen A, Einarsson R, Harlozinska A. *Cancer* 2002;95:1886–1893. [PubMed: 12404282]
- Sokoll LJ, Wians FH, Remaley AT. *Clinical Chemistry* 2004;50:1126–1135. [PubMed: 15117855]
- Sun EY, Weissleder R, Josephson L. *Small* 2006;2:1144–1147. [PubMed: 17193579]
- Takeuchi H, Kitajima M, Kitagawa Y. *Cancer Science* 2008;99:441–450. [PubMed: 18070155]
- van Trommel NE, Massuger LF, Schijf CP, ten Kate-Booij MJ, Sweep FC, Thomas CM. *Journal of Clinical Oncology* 2006;24:52–58. [PubMed: 16382113]
- Viville P, Beauvois S, Lambin G, Lazzaroni R, Bredas JL, Kolev K, Laude L. *Applied Surface Science* 1996;96-8:558–562.
- Wisniewski N, Moussy F, Reichert WM. *Fresenius Journal of Analytical Chemistry* 2000;366:611–621. [PubMed: 11225773]
- Yuan XF, Iijima M, Ishi M, Nagasaki Y. *Langmuir* 2008;24:6903–6909. [PubMed: 18510375]

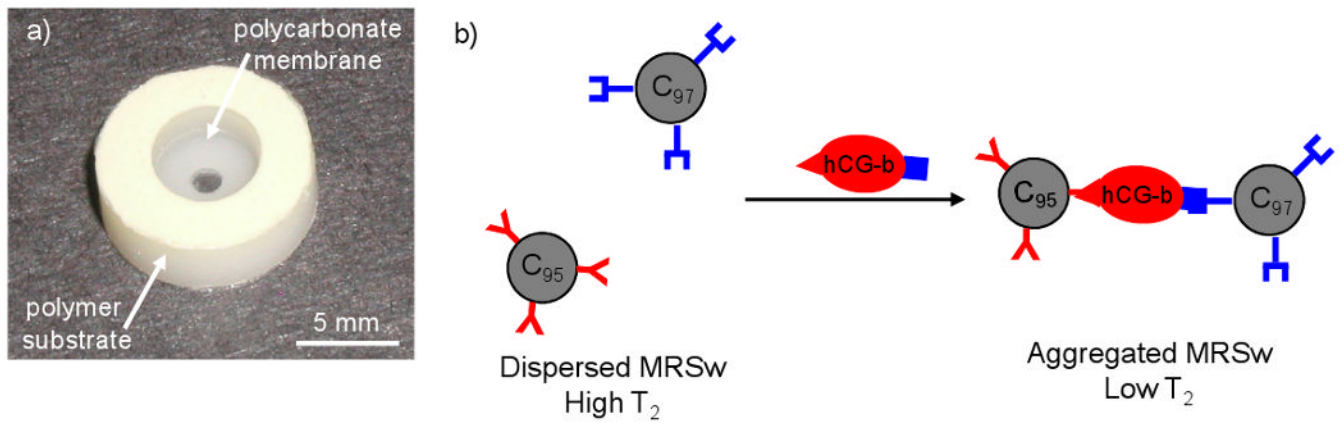


**Figure 1.** Photograph of *in vivo* device (a) and schematic of MRSw aggregation (b). Two populations of MRSw, each functionalized with a different monoclonal antibody for the  $\beta$ -subunit of hCG. Both particle populations must be present for aggregation of the MRSw to occur.

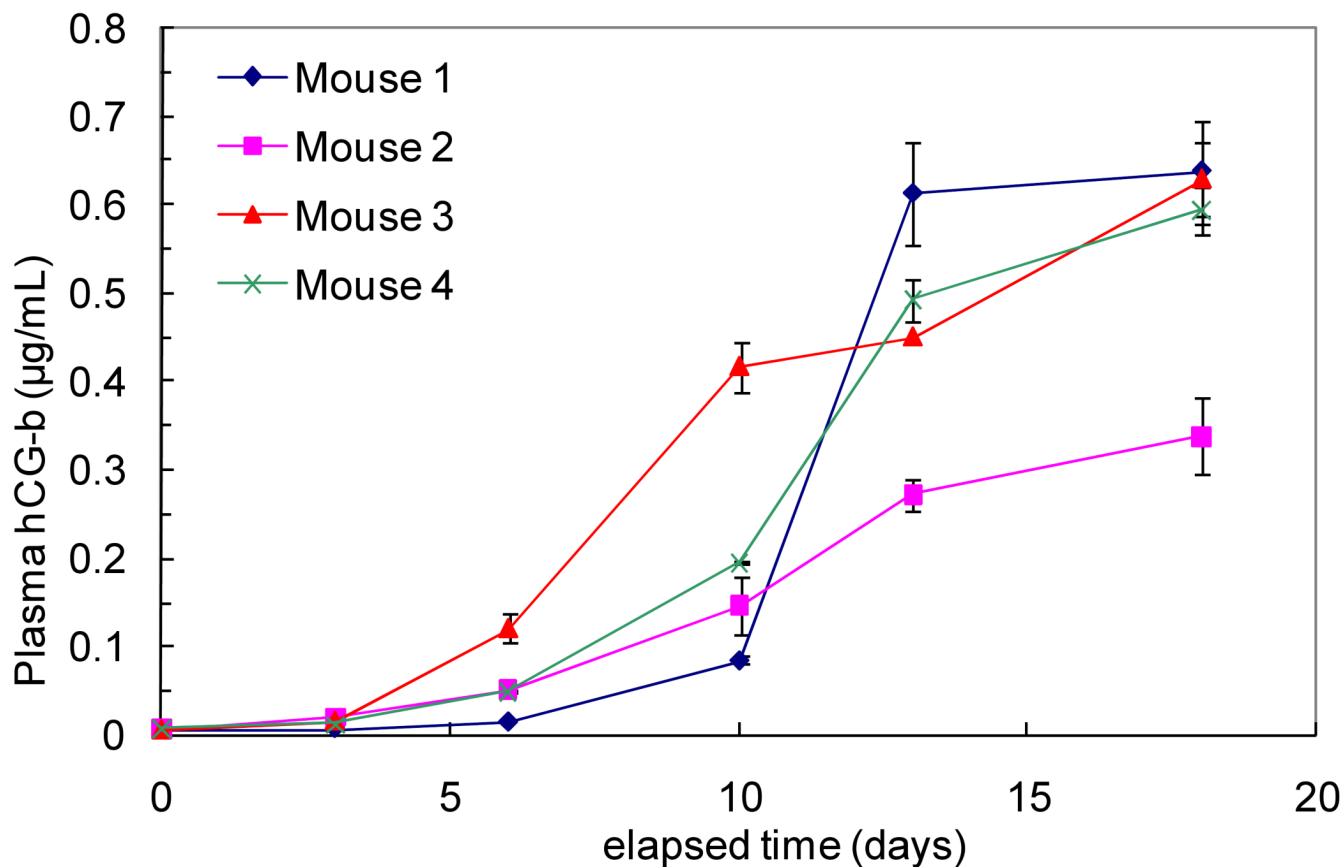


**Figure 2.** hCG- $\beta$  plasma concentration profiles for the first 18 days after tumor induction in four nude mice. Error bars represent standard deviation. hCG- $\beta$  concentrations were quantified using a commercially available ELISA kit. The plasma concentration begins to increase sharply between 7 and 12 days post tumor induction. Previous *in vitro* sensing experiments demonstrated detection of hCG- $\beta$  in a solution with a concentration as low as 0.5  $\mu\text{g/mL}$  (Daniel et al., 2007).

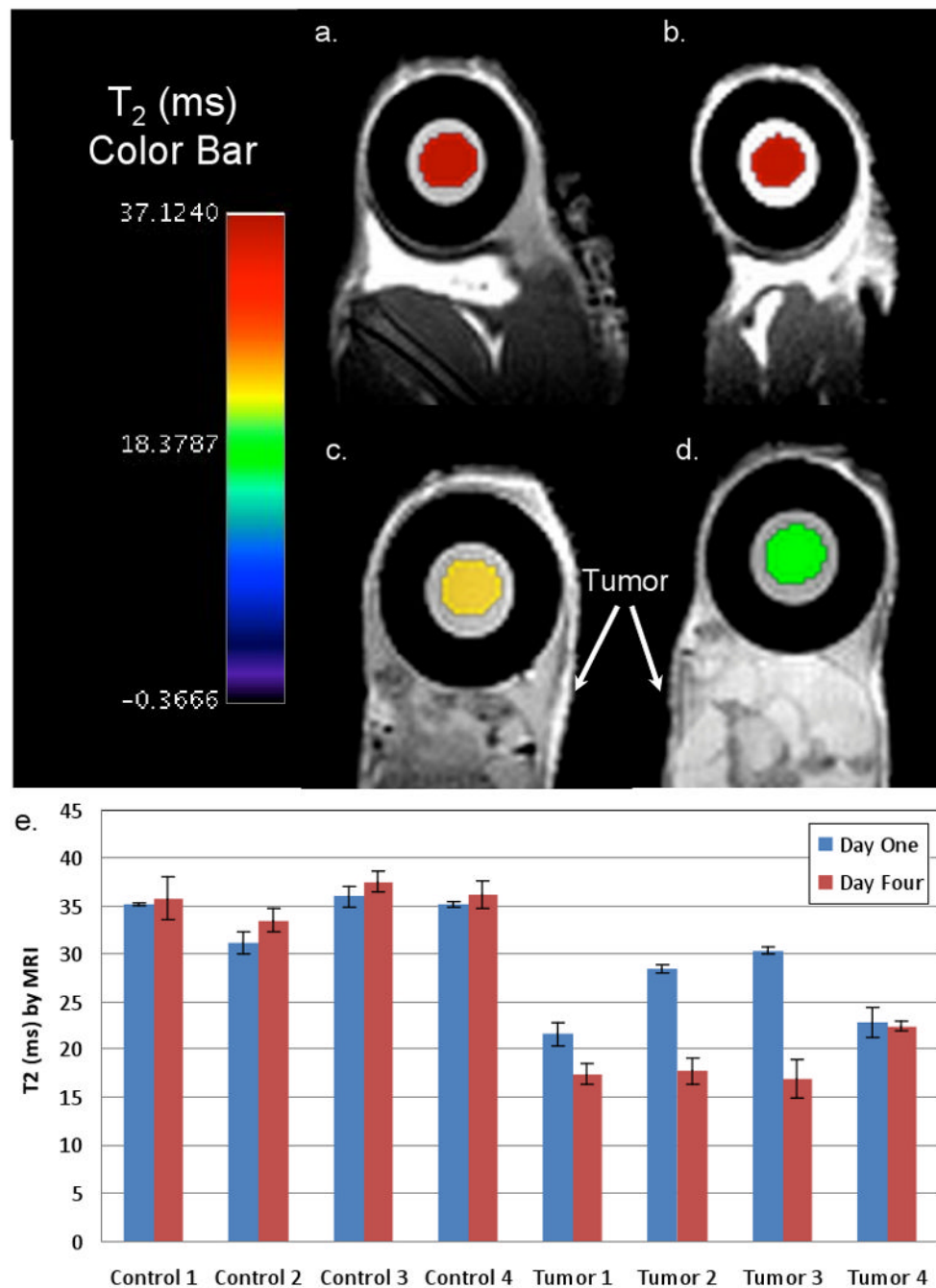


**Figure 3.**

$T_2$ -weighted *in vivo* MR images for a control (a and b) and tumor (c and d) device. Superimposed over the device is a pseudo-colored map of the  $T_2$  within the device (color bar on the left). The control device showed no change in  $T_2$  from day one (a) to day four (b). The  $T_2$  of the sample device decreased from day one (c) to day four (d) and was lower than the control device on both days. e)  $T_2$  values from MR imaging on days one and four post device implantation (error bars represent s.e.m.). The  $T_2$  values of the four control devices are essentially constant over the two time points, indicating that the MRSw did not aggregate or leak from the device.  $T_2$  values for the sample devices are lower than the control devices at both time points.

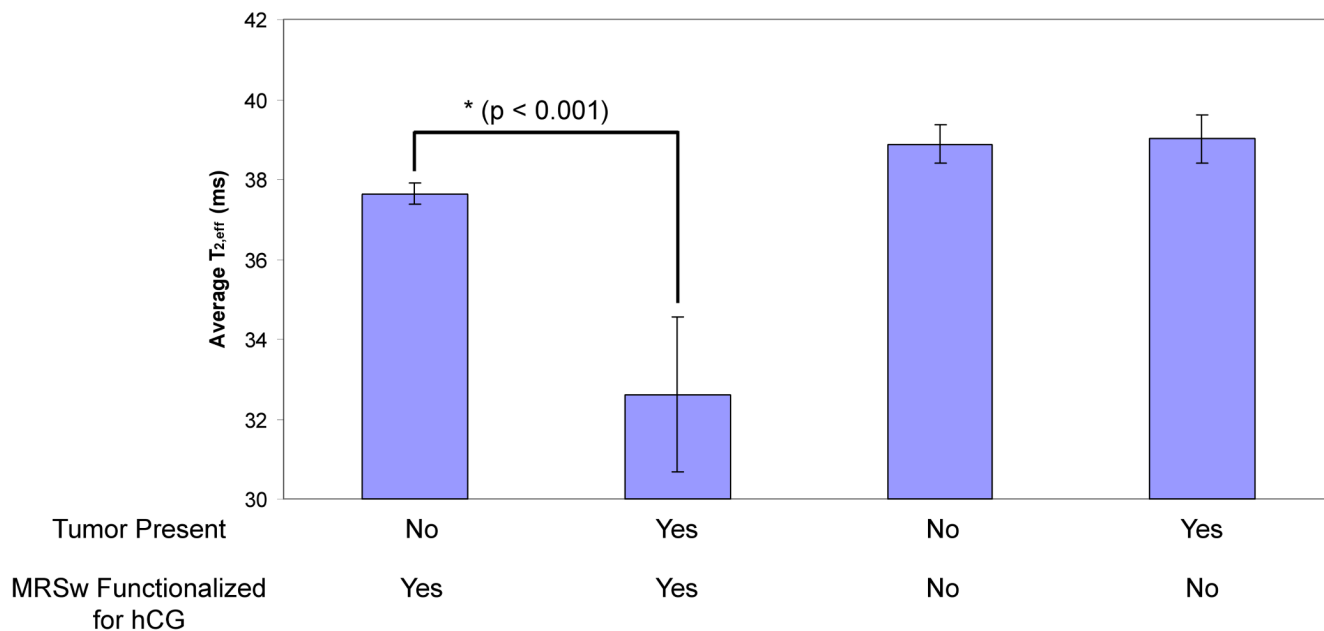


**Figure 4.**

Mean  $T_{2,eff}$  values determined by single-sided MR (error bars represent s.d.) at explant. When devices are filled with MRSw nanoparticles functionalized to detect hCG, there is a statistically significant ( $p < 0.001$ ) decrease in  $T_{2,eff}$  in devices implanted near the tumor ( $n = 19$ ) compared to control devices ( $n = 8$ ) (no tumor). There is no significant change in  $T_{2,eff}$  comparing control ( $n = 6$ ) and sample ( $n = 8$ ) devices, when the devices are filled with non-functionalized nanoparticles.